Evolution of electron temperature in inductively coupled plasma

Hyo-Chang Lee, B. H. Seo, Deuk-Chul Kwon, J. H. Kim, D. J. Seong, S. J. Oh, C.-W. Chung, K. H. You, and ChaeHo Shin

Citation: Appl. Phys. Lett. **110**, 014106 (2017); doi: 10.1063/1.4971980
View online: http://dx.doi.org/10.1063/1.4971980
View Table of Contents: http://aip.scitation.org/toc/apl/110/1
Published by the American Institute of Physics

Evolution of electron temperature in inductively coupled plasma

Hyo-Chang Lee,[1,a)] B. H. Seo,[2] Deuk-Chul Kwon,[3] J. H. Kim,[1,a)] D. J. Seong,[1] S. J. Oh,[4] C.-W. Chung,[4] K. H. You,[1] and ChaeHo Shin[5]
[1]*Center for Vacuum Technology, Korea Research Institute of Standard and Science, Daejeon 305-340, South Korea*
[2]*Applied Physics, California Institute of Technology, Pasadena, California 91125, USA*
[3]*Plasma Technology Research Center, Nation Fusion Research Institute, Gunsan 573-540, South Korea*
[4]*Department of Electrical Engineering, Hanyang University, 17 Haengdang-dong, Seongdong-gu, Seoul 133-791, South Korea*
[5]*Division of Industrial Metrology, Korea Research Institute of Standard and Science, Daejeon 305-340, South Korea*

(Received 6 October 2016; accepted 27 November 2016; published online 6 January 2017)

It is generally recognized that the electron temperature T_e either remains constant or decreases slightly with plasma power (plasma density). This trend can be simply verified using a single-step or multi-step fluid global model. In this work, however, we experimentally observed that T_e evolved with plasma power in radio frequency (RF) inductively coupled plasmas. In this experiment, the measured electron energy distributions were nearly Maxwellian distribution. In the low RF power regime, T_e decreased with increasing plasma power, while it increased with plasma power in the high RF power regime. This evolution of T_e could be understood by considering the coupling effect between neutral gas heating and stepwise ionization. Measurement of gas temperature via laser Rayleigh scattering and calculation of T_e using the kinetic model, considering both multi-step ionization and gas heating, were in good agreement with the measured value of T_e. This result shows that T_e is in a stronger dependence on the plasma power. *Published by AIP Publishing.*
[http://dx.doi.org/10.1063/1.4971980]

Electron temperature (T_e) is one of the most important plasma parameters in both industrial plasma processes and fundamental laboratory research.[1–3] In industrial semiconductor, display, and solar-cell plasma processes, such as etching and deposition, key mechanism for achieving high-quality device fabrication is the physical and chemical reactions. The ion energy/flux impinging on the wafer, which is affected by the T_e, determines the physical reaction. This is because, the sheath potential and the number density of ions change depending on the value of T_e. The radical density and its composition, which are related to the chemical reaction on the wafer surface, are predominantly governed by T_e or electron energy distribution function (EEDF).[4] In laboratory research, T_e is a fundamental plasma parameter that aids in the understanding of the discharge characteristics[5–10] and electron sustainment mechanisms,[11–13] such as electron heating.

It was generally recognized that T_e is decoupled[1,14,15] or slightly coupled[16,17] to the absorbed plasma power (or plasma density n_e) in inductively coupled plasmas (ICPs). In the single–step ionization global model based on fluid analysis, T_e is determined by particle conservation, while n_e is obtained from the power balance equation. Thus, T_e remains unaltered with increasing plasma power or n_e. In the multi-step ionization global model, which uses modified fluid approximation,[16] T_e is slightly decreased with plasma power or n_e, because multi-step ionization caused by excited (mainly metastable) atoms results in a decrease in the collisional energy loss (ε_c) per electron-ion pair created, although the rate of decrease of T_e is significantly low compared to the variation in n_e. Recently, effect of the EEDF was also considered in the global model.[18,19]

In this study, however, we observed an abnormal variation in T_e with the plasma power in ICP, which implies that the T_e is strongly coupled to the plasma power and n_e. This variation in T_e was analyzed via laser Rayleigh scattering measurements and the improved kinetic model considering both multi-step ionization and gas heating.

The experiment was investigated in a radio frequency (RF) ICP reactor (Fig. 1). The chamber had a cylindrical shape with an inner diameter of 26 cm and a height of 18 cm from top plate to bottom electrode. The sidewall and bottom electrode were made of stainless steel, and the top plate was made of ceramic. An RF power of 13.56 MHz was applied to an antenna coil, and an automatically controlled L-type impedance matching network was placed between the RF power generator and the antenna coil to minimize the reflected power. A rotary vane pump and a turbo-molecular vacuum pump were used to maintain the base pressure below 5×10^{-6} Torr. Argon gas was used to sustain the plasma, and the gas flow rate was controlled by a mass flow controller.

To measure the plasma parameters, such as T_e and the electron energy probability function (EEPF), an RF-compensated single Langmuir probe was placed at the center of the discharge region. A schematic of the Langmuir probe configuration can be seen in Refs. 19–21. Briefly describing, the probe had a tip made of tungsten wire with a diameter of 0.1 mm and a length of 6 mm; the probe body was made of a ceramic tube with a telescoping structure.[22] To compensate for the RF fluctuations in the measurement of the current–voltage (I–V) curve, a reference holder and resonance filters

[a)]Authors to whom correspondence should be addressed. Electronic addresses: lhc@kriss.re.kr and jhkim86@kriss.re.kr

corresponding to a fundamental frequency of 13.56 MHz and a second harmonic frequency of 27.12 MHz were included in the Langmuir probe system. The EEPF is obtained by using the AC superposition method.[23–27] This method can offer the reliable EEPF because a small error of the *I-V* curve in the conventional method (direct second derivative method) can give enormous distortion in the EEPF. When a sinusoidal voltage (v_0) is applied to the measured *I–V* curve, the plasma current can be obtained using Taylor series expansion, and the second harmonic current $I_{2\omega}$ is given as $I_{2\omega} \approx \frac{v_0^2}{4}\frac{d^2I(V)}{dV^2}$. Because $\frac{d^2I_e(V)}{dV^2} \gg \frac{d^2I_i(V)}{dV^2}$ except when the probe potential is very close to or larger than the plasma potential,[23,24] $I_{2\omega}$ can be written as

$$I_{2\omega} \approx \frac{v_0^2}{4}\frac{d^2I_e(V)}{dV^2}. \quad (1)$$

Here, $I_e(V)$ and $I_i(V)$ are the electron current and the ion current. Because the EEDF $g_e(\varepsilon)$ is proportional to the second derivative of the electron current $I_e(V)$ in isotropic plasmas[1,28] as $g_e(\varepsilon) = \frac{2m}{e^2A}\left(\frac{2\varepsilon}{m}\right)^{0.5}\frac{d^2I_e(V)}{dV^2}$, the measurement of $I_{2\omega}$ gives the value of EEDF or EEPF. Here, the EEPF $f_e(\varepsilon)$ is related to the $g_e(\varepsilon)$ as $g_e(\varepsilon) = \varepsilon^{0.5}f_e(\varepsilon)$. T_e is obtained from the EEDF as follows:

$$T_e = \frac{2}{3}\frac{1}{n_e}\int_0^\infty \varepsilon g_e(\varepsilon)d\varepsilon, \quad (2)$$

where $n_e = \int_0^\infty g_e(\varepsilon)d\varepsilon$.

Figure 2 shows the measured T_e and EEPF with increasing RF power at an argon gas pressure of 50 mTorr. As the RF power increases, a variation in the trend of T_e was observed. T_e decreased when the RF power increased from 100 W to 500 W, at first. However, T_e increased with a further increase in the RF power. This change in T_e was also found in both discharge center and radial boundary by using the EEPF measurement and floating harmonic technique (not shown here),[29] and the results were in identical trends to Fig. 2. The evolution in T_e is interesting because it was well known that T_e will either remain constant or slightly decrease with n_e in the single-step or multi-step ionization global model.[1,16] One possible explanation for this trend in T_e may be the dramatic evolution of the EEPF through the electron heating effect[11,21,30–37] or electron-electron collisions.[17,26,38,39] However, our experiment was conducted in plasmas having nearly Maxwellian EEPFs. As shown in Fig. 2(b), the measured EEPFs are in the Maxwellian shape except for a slight different tail in the inelastic electron energy range. Therefore, the behavior of T_e is not due to the evolution of the EEPF. In the measured EEPFs, the variation in T_e could also be observed clearly through changes in the slope of the EEPF in elastic electron energy range, which is inversely proportional to T_e.

This evolution of T_e can be understood by coupling effect between neutral gas heating and stepwise ionization. When stepwise ionization is considered in plasmas, the ionization efficiency is enhanced because the ionization energy of the excited atoms is lower than that of the grounded atoms. For example, electron energy of 11.5–11.7 eV is required to excite ground state argon atoms to the metastable state; atoms in the metastable state have a long radiative lifetime compared to other excited state atoms.[1] This means that an additional energy of only about 4–5 eV is needed for the ionization process to initiate, which is much lower than the single collision ionization energy (15.76 eV) of the ground state atoms. Because the stepwise ionization process is enhanced with increasing n_e, ε_c is reduced with an increase in the RF power. Therefore, T_e decreases with an increase in the plasma power in the stepwise ionization model.

However, this model did not account for the effect of the neutral gas heating. The neutral gas is heated by various collisions in the plasma. There are many possible gas-heating mechanisms in noble gas plasmas. One mechanism is electron-neutral collisions. But, electron-neutral collisions may account for only a small fraction of gas heating because in such collisions, the energy transfer ratio is dependent on the mass ratio although T_e is much higher than the gas temperature T_g. In the case of molecular gas plasmas, gas heating due to the energy released in dissociation processes can be significant. The other mechanism is ion-neutral collisions, such as momentum collisions and charge transfer collisions. In these cases, the energy transfer ratio will be very high owing to the similar masses involved although the ion temperature T_i is not high. However, if ion acceleration by ambipolar potential or sheath potential is considered in ion-neutral collisions, a sufficiently strong gas heating effect may occur; this effect becomes more prominent as n_e increases.

The gas heating results in an inverse variation in T_e compared to the variation of T_e via the stepwise ionization because an increase in T_g results in a decrease in the gas density in terms of pressure balance; this causes T_e to increase with increasing n_e. To understand the variation in T_e by this coupling effect between gas heating and stepwise ionization, measurement of T_g using laser Rayleigh scattering and calculation of T_e using the kinetic model considering both multi-step ionization and gas heating were performed.

Figure 3(a) shows the plot of the measured T_g versus RF power obtained using the laser Rayleigh scattering measurement system shown in Fig. 1. The measurement procedure and method can be found in Refs. 40 and 41. The apparatus is described as follows. A frequency-doubled Nd:YAG laser (Powerlite 9010, Continuum, Inc.) with a pulse energy of 300 mJ and a frequency of 10 Hz was used to measure the scattering signals. A laser beam, which is vertically polarized, was focused at the center of the chamber. The scattered signals were collected by the two lenses—the monochromator and the intensified charged coupled device (ICCD) camera (PIMAX, Princeton Instruments). The Rayleigh scattering signals of 2000 shots were accumulated for 200 s. The laser energy was also monitored at the end of the laser path. From the measurements of the Rayleigh scattering signals with and without plasma, T_g can be determined as follows:

$$T_g = T_{ref}\frac{P_{ref} - P_{stray}}{P_{plasma} - P_{stray}}. \quad (3)$$

Here, T_{ref}, P_{ref}, P_{plasma}, and P_{stray} are the room temperature, the wavelength-integrated scattered power of the Rayleigh

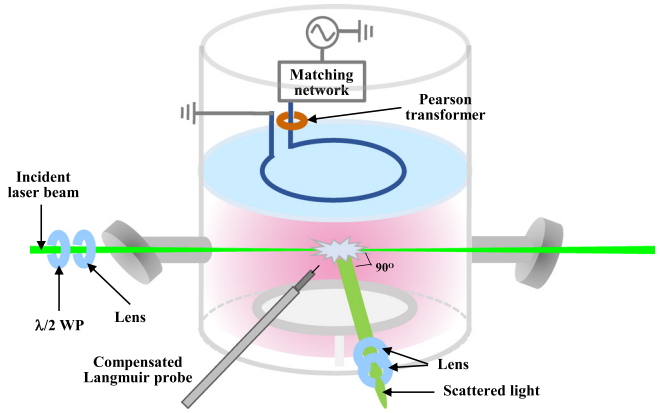

FIG. 1. Experimental setup of an inductively coupled plasma reactor.

signal without plasma as the reference measurement, the wavelength-integrated scattered power of the Rayleigh signal with plasma, and the wavelength integrated scattered power of stray light in a vacuum, respectively. The measured T_g is indicated in Fig. 3(a). When the RF power of 100 W was applied, T_g was approximately 300 K. As the RF power increased from 100 W to 500 W, T_g increased slightly. When more RF power was applied, T_g increased remarkably upto 946 K. This trend in the variation of T_g is in good agreement with other experiments.[42–44]

Figures 3(b) and 3(c) present the measured power absorption and n_e against RF power. When the RF power increased from 100 W to 500 W, n_e increases (Fig. 3(c)) and T_e decreases (Fig. 2(a)) due to enhanced power absorption and stepwise ionization. This increase in the n_e results in the gas heating and thus, the gas temperature is increased (Fig. 3(a)). When more RF power is applied, the n_e reaches to a high plasma density regime as $5 \times 10^{11}\,\mathrm{cm}^{-3}$–$9 \times 10^{11}\,\mathrm{cm}^{-3}$ (Fig. 3(c)), which results in strong gas heating, as shown in Fig. 3(a). Even though the stepwise ionization process also occurs in the high power (high n_e) regime, the remarkable gas heating and high n_e make the neutral density depleted. Therefore, the plasma production is saturated (Fig. 3(c)). It is noted that this behavior makes electron temperature to be increased (Fig. 2(a)) via transition of the discharge characteristics from being stepwise ionization-dominated to gas heating–dominated.

As shown in Figs. 2 and 3, the increase in T_g can significantly affect plasma parameters, such as T_e and n_e. To see this dynamics of the plasma parameters, we numerically solved the global transport equations and the Fokker-Planck equation.[45–49] The global transport equation is given as

$$\frac{\partial n_i}{\partial t} = \sum_j R_{g,j} + \frac{Q_i}{\Omega} - \sum_j R_{l,j} - n_i\left(\frac{V_{pump}}{\Omega} + \nu_l^i\right), \quad (4)$$

where n_i is the density of the species i, Q_i is the gas flow rate of species i, Ω is the volume of the chamber, and V_{pump} is the pumping speed. The loss speed of the ions at the plasma-sheath boundary is assumed to be the Bohm velocity; thus, the loss frequency of the ith ion species becomes $\nu_l^i = A_{eff}\sqrt{T_e/M_i}/\Omega$. Here, M_i is the ion mass and A_{eff} is the effective surface area shown as

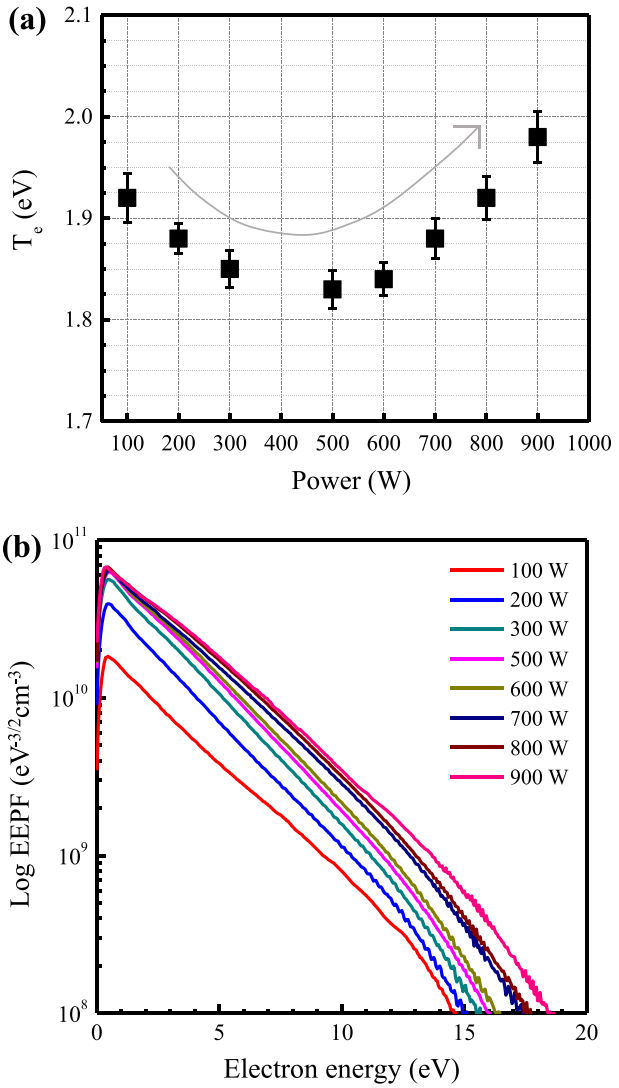

FIG. 2. Experimental results of (a) electron temperature (T_e) and (b) electron energy probability function (EEPF) with RF power.

$$A_{eff} = \frac{n_{is}}{n_i}\bigg|_{\text{axial}} 2\pi R_p^2 + \frac{n_{is}}{n_i}\bigg|_{\text{radial}} 2\pi R_p L_p, \quad (5)$$

where R_p is the plasma radius, L_p is the plasma length, and the ratio of sheath edge density n_{is} to the bulk average density n_i is derived in Refs. 1 and 18. $R_{g,j}$ and $R_{l,j}$ are the reaction rates

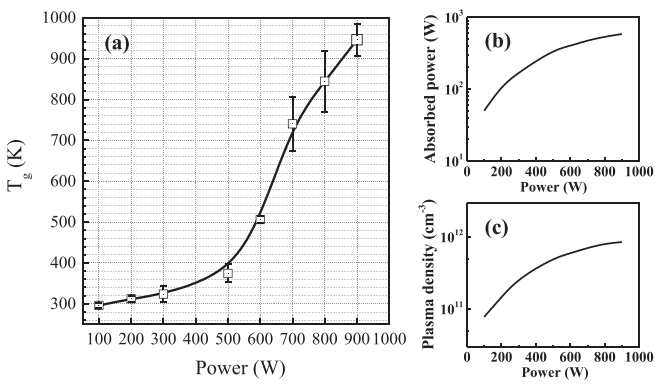

FIG. 3. (a) Measured gas temperature, (b) RF power absorption, and (c) plasma density with RF power.

of the various generation and loss processes of the species i, respectively. In particular, the reaction rates for electron-neutral collisions are calculated as the product of the reactants' densities and the rate coefficient k of the reaction as shown in

$$k = \int_0^\infty f_0(\varepsilon)\sigma(\varepsilon)\upsilon d\varepsilon. \quad (6)$$

Here, $\sigma(\varepsilon)$ is the electron-neutral collision cross sections. In this work, $4s_r$, $4s_m$, and 4p excited states are considered and the reactions are given in Refs. 16 and 19, and radiation trapping[50,51] is not considered in the kinetic model.

It should be noted that our measurement shows Maxwellian EEPFs with depletion on the high-energy part, and the depleted part becomes replenished with RF powers due to the electron-electron collisions. Because the high energy tail on the EEPF can result in change of the stepwise ionization process with the enhanced excitation states, the EEDF should be considered in the model, and the EEDF is calculated from the Fokker-Planck equation as follows

$$\frac{1}{\upsilon}\frac{\partial}{\partial\varepsilon}\upsilon\left[\upsilon(D_\varepsilon + D_{ee} + D_{en})\frac{\partial f_0}{\partial\varepsilon} + (V_{ee} + V_{en})f_0\right] = I, \quad (7)$$

where υ is the electron velocity, D_ε is the energy diffusion coefficient describing electron heating, $D_{ee(n)}$ and $V_{ee(n)}$ are the coefficients of diffusion and dynamic friction caused by electron-electron (neutral) collisions, and I represents inelastic collision including ionization and excitation for Ar discharges.

By solving Eqs. (4)–(7), T_e could be calculated, and the results are indicated in Fig. 4. In the calculation, the measured gas temperature was used, and the effect of variation of T_e by adding the gas temperature on the kinetic model was compared. As not shown here, the calculated EEPFs were in excellent agreement with the measured result: the EEPF shows Maxwellian distribution with a slightly depleted high energy part, and the depleted tail is replenished with the RF power. If we only consider stepwise ionization in the global model, T_e should decrease with an increase in the input power due to the reduction in ε_c by the stepwise ionization, which is represented by dotted lines in Fig. 4. When gas heating is included in the stepwise ionization global model, however, the T_e behavior changes abnormally (solid line in Fig. 4). As observed from the results of the kinetic model considering gas heating, T_e decreases with low RF power at first because of the stepwise ionization. After that, T_e is saturated with an RF power of approximately 300–500 W, which implies that the effects of the stepwise ionization and the gas heating are balanced in the variation in T_e. With a further increase in the RF power, T_e is remarkably increased, and this indicates that the mechanism for the variation of T_e transits from being stepwise ionization–dominated to gas heating–dominated. Therefore, the observed evolution of the T_e is mainly due to the transition of the discharge characteristics owing to the contrasting effects of the stepwise ionization and gas heating. The calculated result (solid line in Fig. 4) using the kinetic model including both the stepwise ionization and gas heating is in good agreement with the experimental result shown in Fig. 2(a).

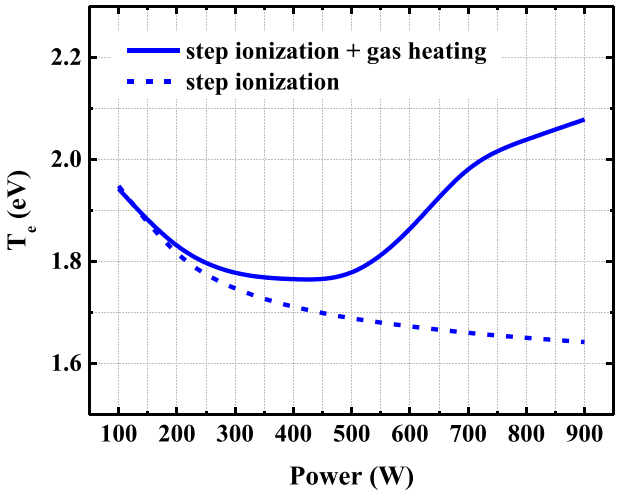

FIG. 4. Calculated electron temperature using the kinetic model with and without gas heating.

In this letter, we observed the abnormal behavior of T_e in ICP. In the low RF power or plasma density region, T_e decreased, while it remarkably increased in the high RF power region. It was also demonstrated from the laser Rayleigh scattering measurement that T_g slightly increased with low RF powers, and it significantly increased in the high RF power region. The kinetic model, which considers stepwise ionization and gas heating, was developed to analyze the change in T_e. From the kinetic model analysis, the apparently abnormal trend in T_e can be understood by the contrasting effects of stepwise ionization and gas heating. It should be noted that the original notion was that T_e is decoupled (or weakly coupled) to the plasma power or plasma density, and thus, T_e must remain constant (or slightly decrease) with plasma density in the conventional global model. However, our experiments and improved modeling show that T_e has a much stronger relationship with plasma power than we initially expected, and the gas heating effect should be considered.

The authors thank anonymous reviewers. This research was supported by Korea Research Institute of Standard and Science (KRISS) and the R&D Convergence Program (CAP-16-04-KRISS) of National Research Council of Science and Technology (NST) of Republic of Korea, and also supported by R&D Program of "Plasma BigData ICT Convergence Technology Research Project" through the National Fusion Research Institute of Korea (NFRI) funded by the Government funds.

[1]M. A. Lieberman and A. J. Lichtenberg, *Principle of Plasma Discharges and Materials Processing* (Wiley, New York, 2005).
[2]F. Chen, *Introduction to Plasma Physics and Controlled Fusion: I. Plasma Physics*, 2nd ed. (Plenum, New York, 1984).
[3]P. Chabert and N. Braithwaite, *Physics of Radiofrequency Plasmas* (Cambridge University Press, Cambridge, 2011).
[4]H.-C. Lee and C.-W. Chung, Plasma Sources Sci. Technol. **23**, 062002 (2014).
[5]K. Takahashi, C. Charles, R. W. Boswell, and T. Fujiwara, Phys. Rev. Lett. **107**, 035002 (2011).
[6]V. A. Godyak and R. B. Piejak, Appl. Phys. Lett. **63**, 3137 (1993).
[7]M. J. Hartig and M. J. Kushner, J. Appl. Phys. **73**, 1080 (1993).

[8]J. Schulze, T. Gans, D. O'Connell, U. Czarnetzki1, A. R. Ellingboe, and M. M. Turner, J. Phys. D: Appl. Phys. **40**, 7008 (2007).
[9]H.-C. Lee, M.-H. Lee, and C.-W. Chung, Appl. Phys. Lett. **96**, 041503 (2010).
[10]S. Park, W. Choe, S. Y. Moon, and J. Park, Appl. Phys. Lett. **104**, 084103 (2014).
[11]V. A. Godyak and R. B. Piejak, Phys. Rev. Lett. **65**, 996 (1990).
[12]M. M. Turner, D. A. W. Hutchinson, R. A. Doyle, and M. B. Hopkins, Phys. Rev. Lett. **76**, 2069 (1996).
[13]H.-C. Lee and C.-W. Chung, Appl. Phys. Lett. **101**, 244104 (2012).
[14]C. Lee and M. A. Lieberman, J. Vac. Sci. Technol., A **13**, 368 (1995).
[15]P. N. Wainman, M. A. Lieberman, A. J. Lichtenberg, R. A. Stewart, and C. Lee, J. Vac. Sci. Technol., A **13**, 2464 (1995).
[16]M.-H. Lee and C.-W. Chung, Appl. Phys. Lett. **87**, 131502 (2005).
[17]V. A. Godyak, R. B. Piejak, and B. M. Alexandrovich, Plasma Sources Sci. Technol. **11**, 525 (2002).
[18]J. T. Gudmundsson, Plasma Sources Sci. Technol. **10**, 76 (2001).
[19]H.-C. Lee and C.-W. Chung, Sci. Rep. **5**, 15254 (2015).
[20]H.-C. Lee and C.-W. Chung, Phys. Plasmas **19**, 033514 (2012).
[21]H.-C. Lee and C.-W. Chung, Phys. Plasmas **20**, 101607 (2013).
[22]V. A. Godyak and V. I. Demidov, J. Phys. D: Appl. Phys. **44**, 269501 (2011).
[23]R. Boyd, Proc. R. Soc., A **201**, 329 (1950).
[24]R. Boyd and N. Twiddy, Proc. R. Soc., A **250**, 53 (1959).
[25]R. H. Sloane and E. I. R. MacGregor, Philos. Mag. **18**, 193 (1934).
[26]S. H. Seo, C. W. Chung, J. I. Hong, and H. Y. Chang, Phys. Rev. E **62**, 7155 (2000).
[27]H.-C. Lee, H.-J. Hwang, Y.-C. Kim, J. Y. Kim, D.-H. Kim, and C.-W. Chung, Phys. Plasmas **20**, 033504 (2013).
[28]M. J. Druyvesteyn, Z. Phys. A. Hadrons and Nuclei **64**, 781 (1930).
[29]D. Kim, H.-C. Lee, Y. Kim, and C. Chung, Appl. Phys. Lett. **103**, 084103 (2013).
[30]V. A. Godyak, R. B. Piejak, and B. M. Alexandrovich, Phys. Rev. Lett. **68**, 40 (1992).
[31]O. V. Polomarova, C. E. Theodosiou, and I. D. Kaganovich, Phys. Plasmas **12**, 080704 (2005).
[32]I. V. Schweigert, Phys. Rev. Lett. **92**, 155001 (2004).
[33]E. Schüngel, S. Brandt, Z. Donkó, I. Korolov, A. Derzsi, and J. Schulze, Plasma Sources Sci. Technol. **24**, 044009 (2015).
[34]J. Schulze, E. Schüngel, Z. Donkó, and U. Czarnetzki, Plasma Sources Sci. Technol. **20**, 015017 (2011).
[35]H.-C. Lee and C.-W. Chung, Plasma Sources Sci. Technol. **24**, 024001 (2015).
[36]A. V. Khrabrov, I. D. Kaganovich, P. L. G. Ventzek, A. Ranjan, and L. Chen, Plasma Sources Sci. Technol. **24**, 054003 (2015).
[37]Y.-X. Liu, Q.-Z. Zhang, W. Jiang, L.-J. Hou, X.-Z. Jiang, W.-Q. Lu, and Y.-N. Wang, Phys. Rev. Lett. **107**, 055002 (2011).
[38]H.-C. Lee, J.-K. Lee, and C.-W. Chung, Phys. Plasmas **17**, 033506 (2010).
[39]V. A. Godyak and B. M. Alexandrovich, J. Appl. Phys. **118**, 233302 (2015).
[40]B. H. Seo, S. J. You, and J. H. Kim, Jpn. J. Appl. Phys., Part 1 **54**, 086102 (2015).
[41]B. H. Seo, D. W. Kim, J. H. Kim, and S. J. You, Phys. Plasmas **22**, 093510 (2015).
[42]V. M. Donnelly and M. V. Malyshev, Appl. Phys. Lett. **77**, 2467 (2000).
[43]G. A. Hebner, J. Appl. Phys. **80**, 2624 (1996).
[44]G. Cunge, D. Vempaire, and N. Sadeghi, Appl. Phys. Lett. **96**, 131501 (2010).
[45]S. S. Kim, C. W. Chung, and H. Y. Chang, Thin Solid Films **435**, 72 (2003).
[46]S. Ashida, C. Lee, and M. A. Lieberman, J. Vac. Sci. Technol., A **13**, 2498 (1995).
[47]F. Kannari, M. Obaraa, and T. Fujioka, J. Appl. Phys. **57**, 4309 (1985).
[48]N. L. Bassett and D. J. Economou, J. Appl. Phys. **75**, 1931 (1994).
[49]D. R. Lide, *CRC Handbook of Chemistry and Physics*, 80th ed. (CRC Press, Boca Raton, 2000).
[50]M. Schulze, A. Yanguas-Gil1, A. Keudell, and P. Awakowicz, J. Phys. D: Appl. Phys. **41**, 065206 (2008).
[51]N. Kang, S. Oh, and A. Ricard, J. Phys. D: Appl. Phys. **41**, 155203 (2008).